PERGAMON

International Journal of Multiphase Flow 27 (2001) 2015–2021

International Journal of Multiphase Flow

www.elsevier.com/locate/ijmulflow

Brief Communication

A note on separation of a bimodal mixture in pipe flow

H.P. Greenspan [a,*], M.S. Nigam [b]

[a] *Department of Mathematics, Massachusetts Institute of Technology, Cambridge, MA 02139, USA*
[b] *BP Institute for Multiphase Flow, Madingley Rise, Madingley Road, Cambridge CB3 0EZ, UK*

Received 2 November 2000; received in revised form 3 July 2001

1. Introduction

The theory of particle/fluid mixtures, practically speaking, is really a set of model equations which attempts to incorporate the major effects of particle interactions as guided by experimental findings. A reasonable basis now exists for the theoretical description of the particle "collision" (Leighton and Acrivos, 1987a,b; Phillips et al., 1992) caused by gradients of shear rate, viscosity and volume fraction. Recently, and in order to explain certain experimental results with viscometers, collisions due to the changing curvature of particle paths have been postulated (Krishnan et al., 1996). Although this model seems to yield good agreement with experiments (Shauly et al., 1998), the physical basis of these interactions needs further elucidation. As the results of new experiments are reported, especially those with particles of different sizes, other modifications, additions and elaborations of the model will undoubtedly be required. One effect for consideration here is that the smaller particles have much longer and more deviant paths of motion (relative to their diameters) as they move about the larger elements of the mixture. For this reason, the irreversible processes of collisions must have a greater effect per unit time on the smaller particles which implies a diffusion that for each species is dependent on the particle diameter of the other. The flow of a mixture in a pipe is considered anew from this postulation.

2. Formulation

The model equations for the motion of a non-dilute, neutrally buoyant mixture of spherical particles of just two different sizes, are modifications of those used by Shauly et al. (1998). Essentially there are equations for the conservation of each particle species:

* Corresponding author. Tel.: +1-617-253-4982.
E-mail address: hpg@math.mit.edu (H.P. Greenspan).

PII: S0301-9322(01)00047-7

$$\frac{\partial \phi_1}{\partial t} + \nabla \cdot \phi_1 \mathbf{v}_{d1} = 0, \tag{1}$$

$$\frac{\partial \phi_2}{\partial t} + \nabla \cdot \phi_2 \mathbf{v}_{d2} = 0, \tag{2}$$

$$-\frac{\partial \phi}{\partial t} + \nabla \cdot (1-\phi)\mathbf{v}_{\mathrm{C}} = 0, \tag{3}$$

where ϕ_k is the volume fraction, $\mathbf{v}_{dk}$ is the velocity of species k and $\mathbf{v}_{\mathrm{C}}$ is the velocity of the continuous fluid phase. Together these yield

$$\nabla \cdot \mathbf{j} = 0 \tag{4}$$

with $\phi = \phi_1 + \phi_2$ and $\mathbf{j} = \phi_1 \mathbf{v}_{d1} + \phi_2 \mathbf{v}_{d2} + (1-\phi)\mathbf{v}_{\mathrm{C}}$ defines the volume averaged velocity. Constitutive equations for the velocities are then taken to be

$$\mathbf{v}_{d1} = \mathbf{j} - \phi\dot{\gamma}\bar{a}a_1\left(\frac{K_{\mathrm{c}}\nabla\phi\dot{\gamma}}{\phi\dot{\gamma}} + \frac{K_\eta \nabla\eta}{\eta}\right) - \beta(\dot{\gamma},\eta)|a_2 - a_1|a_2\phi_2\nabla\phi_1, \tag{5}$$

$$\mathbf{v}_{d2} = \mathbf{j} - \phi\dot{\gamma}\bar{a}a_2\left(\frac{K_{\mathrm{c}}\nabla\phi\dot{\gamma}}{\phi\dot{\gamma}} + \frac{K_\eta \nabla\eta}{\eta}\right) - \beta(\dot{\gamma},\eta)|a_2 - a_1|a_1\phi_1\nabla\phi_2, \tag{6}$$

where $\dot{\gamma}$ is the strain rate of the volume averaged velocity field, $a_{1,2}$ is the radius of each particle species and $\bar{a} = (a_1\phi_1 + a_2\phi_2)/\phi$ is the scattering length associated with mean mixture quantities. The particles are assumed to be neutrally buoyant. The last term of each equation describes the additional interaction flux due to size differences of the particle species and consequently, the greater frequency of collisions and increased dispersion of the smaller versus the larger particles of the mixture. For simplicity, this flux is assumed to depend directly on the volume fraction and particle diameter of the other component, the absolute difference in sizes and a function involving the mixture strain rate and viscosity. Three separate expressions for $\beta(\dot{\gamma},\eta)$ have been considered,

$$\beta(\dot{\gamma},\eta) = \begin{cases} \beta_1, \\ \beta_2\eta_{\mathrm{C}}/\eta, \\ \beta_3\dot{\gamma}\eta_{\mathrm{C}}/\eta. \end{cases} \tag{7}$$

For slow motions, the momentum equation is

$$-\nabla p + \nabla \cdot \mathbf{\Pi} = \mathbf{0} \tag{8}$$

with the stress tensor given in terms of the rate of strain tensor (of the volume flux field!) by

$$\mathbf{\Pi} = \eta\dot{\boldsymbol{\gamma}}, \tag{9}$$

where $\dot{\gamma} = (\frac{1}{2}\dot{\boldsymbol{\gamma}} : \dot{\boldsymbol{\gamma}})^{1/2}$ and the viscosity of the mixture is

$$\eta = \eta_{\mathrm{C}}\left(1 - \frac{\phi}{\phi_m}\right)^{-1.82} \tag{10}$$

and

$$\frac{\phi_m}{\phi_{m0}} = 1 + 1.5\left|\frac{a_2 - a_1}{a_2 + a_1}\right|^{1.5}\left(\frac{\phi_2}{\phi}\right)^{1.5}\left(\frac{\phi_1}{\phi}\right). \tag{11}$$

A semi-empirical correlation for the effective viscosity (10), suggested by Krieger (1972), is here combined with an expression for the maximum packing concentration (Eq. (11)), based on the experiments of Probstein et al. (1994). The value $\phi_{m0} = 0.68$ was used in the numerical computations presented in the following section.

3. Results

For steady flow of a neutrally buoyant bimodal mixture in a straight cylindrical pipe, the time independent equations must be solved subject to the boundary conditions that there is zero radial flux of either component at the wall of the pipe and all quantities are bounded in the interior flow:

$$\phi_1 \mathbf{v}_{d1} \cdot \hat{\mathbf{r}} = \phi_2 \mathbf{v}_{d2} \cdot \hat{\mathbf{r}} = 0 \quad \text{at } r = 1. \tag{12}$$

The pressure gradient along the pipe is a constant, $p_z = -M$, and since all other quantities are functions only of the radius r, the equations reduce to a set of ordinary differential equations which are readily solved numerically, and even analytically if a few simplifying approximations are made. For example, let the two particle diameters be very different so that $a_1/a_2 \ll 1$. It follows that to lowest order in this parameter, ϕ_1 is uniform across the pipe and equal to the value at the wall

$$\phi_1 = \phi_{1\mathrm{w}}. \tag{13}$$

The equation for the second component reduces to

$$K_\mathrm{c}\frac{\mathrm{d}}{\mathrm{d}r}\log\phi\dot{\gamma} + K_\eta\frac{\mathrm{d}}{\mathrm{d}r}\log\eta = 0, \tag{14}$$

which for the currently accepted values, $K_\mathrm{c} = K_\eta/2$, integrates to

$$\phi\dot{\gamma}\eta^2 = \phi_\mathrm{w}\dot{\gamma}_\mathrm{w}\eta_\mathrm{w}^2. \tag{15}$$

Since $\dot{\gamma} = |w_r| = -w_r = -(\mathrm{d}/\mathrm{d}r)\hat{\mathbf{k}} \cdot \mathbf{j}$, and $\dot{\gamma} \to 0$ as $r \to 0$, the viscosity of the mixture must become infinite at the center which implies maximum volume packing. Since ϕ_1 is constant, ϕ_2 must increase towards the center of the pipe. The conclusion of this simple analysis is that there is a separation of the two species – large particles migrate to the central region, small particles are more uniformly distributed across the cylinder. In simple terms, the small particles act more like molecules and together with the fluid form a "continuous" medium of increased viscosity in which the large particles move.

Further analytical development of the theory leads to simple formulas for all variables, but because the basic equations are integrated numerically without approximations regarding relative particle sizes, only those results are presented in the interests of brevity.

The numerical results depicted in Figs. 1–5 were obtained by integrating the steady-state equations for ϕ_1 and ϕ_2 subject to wall conditions ($\phi_{1\mathrm{w}}$, $\phi_{2\mathrm{w}}$) for the three different β-functions. The boundary conditions $\phi_{1\mathrm{w}}$ and $\phi_{2\mathrm{w}}$ were determined implicitly by specifying the average volume fraction of each species

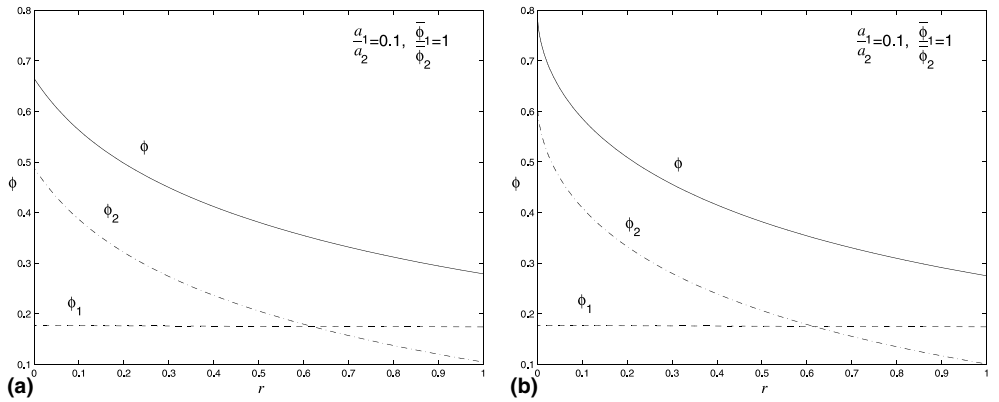

Fig. 1. Steady-state radial concentration profiles for (a) model 1 and (b) model 3. Solid, dashed and dash-dotted curves correspond to ϕ, ϕ_1 and ϕ_2, respectively. The parameters used in the computations were: $a_1/a_2 = 0.1$, $D_{12} = 1.0$, $\bar{\phi}_1/\bar{\phi}_2 = 1.0$ and $\bar{\phi} = 0.35$.

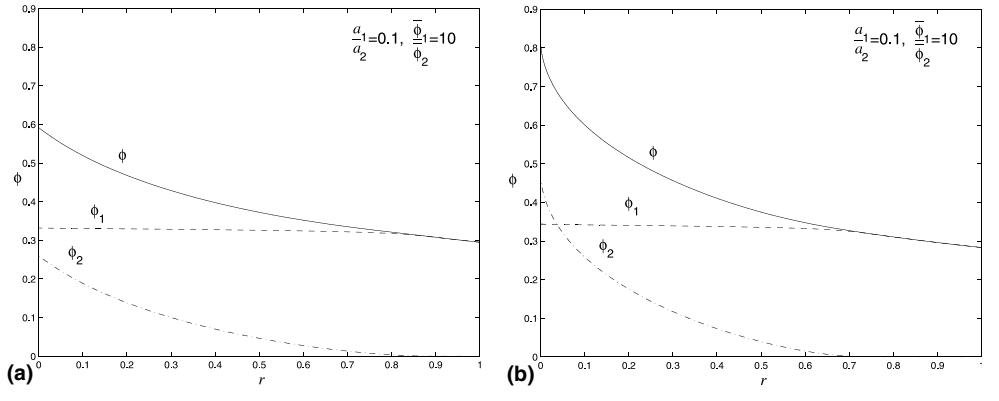

Fig. 2. Steady-state radial concentration profiles for (a) model 1 and (b) model 3. Solid, dashed and dash-dotted curves correspond to ϕ, ϕ_1 and ϕ_2, respectively. The parameters used in the computations were: $a_1/a_2 = 0.1$, $D_{12} = 1.0$, $\bar{\phi}_1/\bar{\phi}_2 = 10$ and $\bar{\phi} = 0.35$.

$$\bar{\phi}_{1,2} = 2\int_0^1 \phi_{1,2}(r) r \, \mathrm{d}r. \tag{16}$$

In addition, transient profiles were obtained by solving the time dependent initial value problem defined in Section 2. In each case, the steady-state profiles agreed with those of the steady computations to within the discretisation error of the numerical method. The steady computations were performed using a variable-step Runge–Kutta method, and a Galerkin finite element discretisation was applied to the transient problem. The details of the numerical schemes will be presented elsewhere (Nigam, in preparation). The non-dimensional parameter measuring the relative influence of the additional flux terms is $D_{12} = 4\beta_{1,2}\eta_C/(K_\eta MR)$ for the first two models, where R is the radius of the pipe, and $D_{12} = 2\beta_3/K_\eta$ for the third model. For moderate values of this parameter, the effect of the β terms is mainly to enforce Eq. (17) below, and the differences

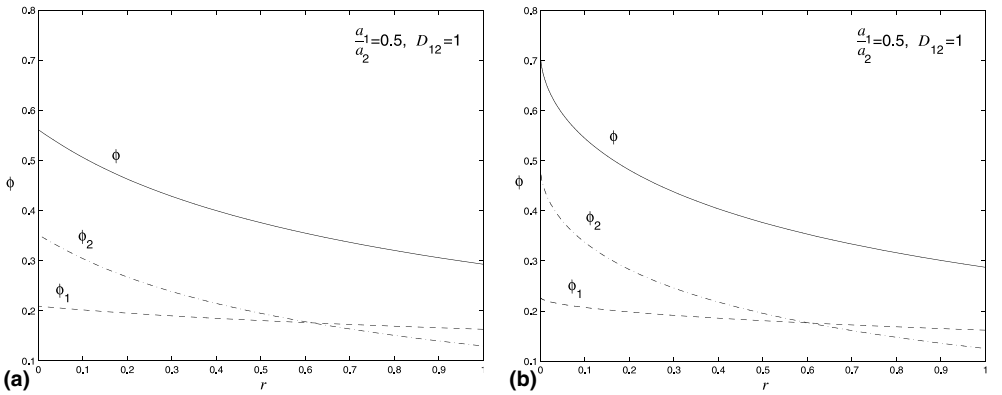

Fig. 3. Steady-state radial concentration profiles for (a) model 1 and (b) model 3. Solid, dashed and dash-dotted curves correspond to ϕ, ϕ_1 and ϕ_2, respectively. The parameters used in the computations were: $a_1/a_2 = 0.5$, $D_{12} = 1.0$, $\bar{\phi}_1/\bar{\phi}_2 = 1.0$ and $\bar{\phi} = 0.35$.

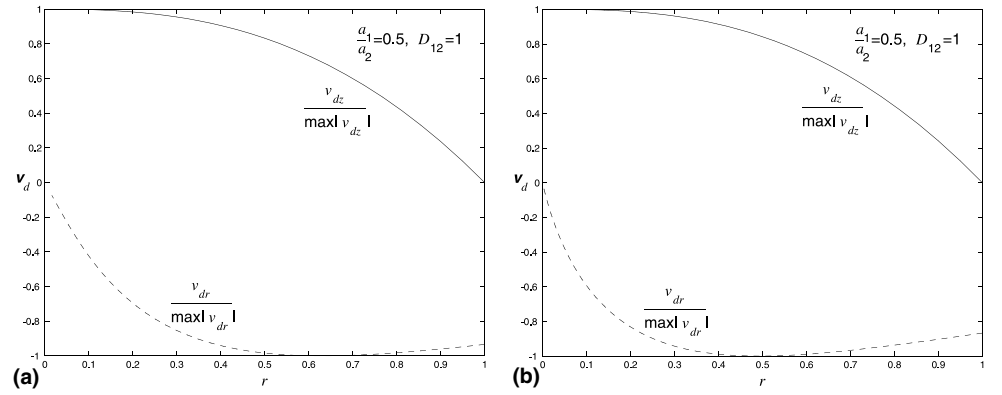

Fig. 4. Normalized radial and axial particle velocity profiles corresponding to Fig. 3 for (a) model 1 and (b) model 3. The axial profiles are the same for both species and the radial profiles are related through $v_{dr1} = (a_1/a_2)v_{dr2}$. The parameters used in the computations were: $a_1/a_2 = 0.5$, $D_{12} = 1.0$, $\bar{\phi}_1/\bar{\phi}_2 = 1.0$ and $\bar{\phi} = 0.35$.

between the steady-state results of models 2 and 3 are indistinguishable. Hence, only the results of the latter model are presented.

Figs. 1(a) and (b) verify the main predictions of the asymptotic analysis. The larger particles migrate as in a unimodal suspension (Phillips et al., 1992). An interesting phenomenon can be observed in Figs. 2(a) and (b). When the ratio of the fine-to-coarse mean volume fractions is increased, the coarse particles are forced towards the center of the pipe. Thus, a unimodal layer of fine particles appears in the vicinity of the outer wall. The strong dependence on the particle size ratio can be understood by looking at the governing equations. For pipe flow, the following exact result is readily obtained for any non-zero value of D_{12}

$$\frac{\phi_1}{\phi_{1\mathrm{w}}} = \left(\frac{\phi_2}{\phi_{2\mathrm{w}}}\right)^{a_1^2/a_2^2}. \tag{17}$$

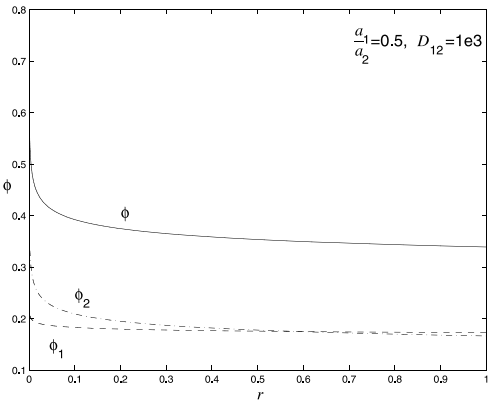

Fig. 5. Steady-state radial concentration profiles for model 3. Solid, dashed and dash-dotted curves correspond to ϕ, ϕ_1 and ϕ_2, respectively. The parameters used in the computations were: $a_1/a_2 = 0.5$, $\bar{\phi} = 0.35$, $\bar{\phi}_1/\bar{\phi}_2 = 1.0$ and $D_{12} = 1000$.

For larger values of the particle size ratio, the differences between the models become more pronounced (Figs. 3(a) and (b)). As the center of the pipe is approached, the influence of the additional flux terms weakens for model 2 due to an increase in concentration, and even faster so for model 3 because of the combined effect with a decreasing shear rate. In fact, the latter model predicts a maximum packing concentration at the center of the pipe. In the first model, on the other hand, the β-terms dominate at the center of the pipe, and the resulting concentration gradients become weaker. The corresponding normalized radial and axial particle velocity profiles are shown in Figs. 4(a) and (b). Note that the steady-state radial particle velocity profiles for the two species only differ by the constant factor a_1/a_2.

In contrast to the strong dependence on the particle size ratio, the dependence on D_{12} is relatively weak. For the first two models, the β-terms are active even in the absence of a flow, and the corresponding coefficients, D_{12}, must therefore be restricted to small values. This restriction does not apply to the third model, and for large values of the parameter the volume fraction profiles develop a boundary layer structure near the center of the pipe (Fig. 5).

4. Conclusions

Numerical results clearly show the adequacy of the simple theoretical analysis. Over an extremely wide range of parameter space, substantial particle separation occurs in a bimodal mixture when the diameters of the two species differ by an order of magnitude – and this is a conservative estimate. Essentially, the larger particles move in a continuum composed of liquid with a uniformly dispersed, "molecular" constituent of the small particle, both together forming a mixture of higher viscosity. This is consistent with the views and findings of Probstein et al. (1994) who have used bimodal approximations of even more complicated mixtures to good effect. Experimental evidence for radial size segregation of a bimodal suspension in pipe flow has been provided by Husband et al. (1994). Their data indicated that the increase in total solids

concentration near the center of the pipe always is accompanied by an increase in the relative amount of coarse-to-fine particles. A closer look at the multi-modal formulation by Shauly et al. (1998) reveals that this model instead predicts that the larger species is more uniformly distributed for pipe flow.

Although the results obtained here are consistent with the limited experimental data available, more definitive experiments are required in this regard to assert more or to determine the magnitude of the various parameters introduced.

An important question, not resolved by the current model, is that some of the cases predict a maximum packing concentration at the center of the pipe, caused by a zero shear rate. Including the effects of a finite particle size on the shear rate would presumably prevent this from occurring (Shauly et al., 1998). Another modification of the basic theory that requires attention, although the improvement in most circumstances may be minor, is the replacement of the fluid strain rate, based on the mass averaged or volume flux velocity fields, with one based on the particle velocity field instead. Collision rates must entail the relative velocities of the particles with each other but such an inclusion has not been considered as yet.

References

Husband, D.M., Mondy, L.A., Ganani, E., Graham, A.L., 1994. Direct measurements of shear-induced particle migration in suspensions of bimodal spheres. Rheol. Acta 33, 185–192.

Krishnan, G.P., Beimfohr, S., Leighton, D., 1996. Shear-induced radial segregation in bidisperse suspensions. J. Fluid Mech. 321, 371–393.

Krieger, I.M., 1972. Rheology of monodisperse latices. Adv. Colloid Interface Sci. 3, 111–136.

Leighton, D., Acrivos, A., 1987a. Measurements of shear-induced self-diffusion in concentrated suspensions of spheres. J. Fluid Mech. 177, 109–131.

Leighton, D., Acrivos, A., 1987b. The shear-induced migration of particles in concentrated suspensions. J. Fluid Mech. 181, 415–439.

Nigam, M.S., in preparation. Transient computations of mixture flow in pipes.

Phillips, R.J., Armstrong, R.C., Brown, R.A., 1992. A constitutive equation for concentrated suspensions that accounts for shear-induced particle migration. Phys. Fluids A 4, 30–40.

Probstein, R.F., Sengun, M.Z., Tseng, T.C., 1994. Bimodal model of concentrated suspension viscosity for distributed particle sizes. J. Rheol. 38, 811–829.

Shauly, A., Wachs, A., Nir, A., 1998. Shear-induced particle migration in a polydisperse concentrated suspension. J. Rheol. 42, 1329–1348.